Lean premixed reacting flows with swirl and wall-separation zones in a contracting open circular chamber

Zvi Rusak,* Yuxin Zhang, and Jung J. Choi
Department of Mechanical, Aerospace and Nuclear Engineering, Rensselaer Polytechnic Institute, Troy, New York 12180, USA

Shixiao Wang
Department of Mathematics, University of Auckland, 38 Princes Street, Auckland 1142, New Zealand

(Received 14 March 2018; published 6 November 2018)

A model problem of low-Mach-number lean premixed reacting swirling flows with wall-separation zones in a contracting circular finite-length open chamber is studied. Assuming a complete reaction with high activation energy and chemical equilibrium behind the reaction zone, a nonlinear partial differential equation is derived for the solution of the flow stream function behind the reaction zone in terms of the specific total enthalpy for a reacting flow, the specific entropy, and the circulation functions prescribed at the chamber's inlet. Four types of solutions of the resulting ordinary differential equation for the columnar flow case describe the outlet state of the flow in a long chamber. The bifurcation diagrams of steady flows as the inlet swirl level is increased at fixed chamber contraction and reaction heat release are described. The approach is applied to an inlet solid-body rotation flow with constant profiles of the axial velocity, temperature, and mixture reactant mass fraction. The computed results provide theoretical predictions of the critical inlet swirl levels for the first appearance of wall-separation states and for the size of the separation zone as a function of the inlet swirl ratio, Mach number, chamber contraction, and heat release of the reaction. The methodology developed in this paper provides a theoretical feasibility for the development of the technology of swirl-assisted combustion where the reaction zone is supported and stabilized by a wall-separation zone.

DOI: 10.1103/PhysRevFluids.3.113201

I. INTRODUCTION

Swirling flows are used in most modern lean-premixed combustion systems to stabilize flames; see, for example, the pioneering papers of Gupta *et al.* [1], Lefebvre [2], Sivasegaram and Whitelaw [3], and Paschereit *et al.* [4,5] that were followed up by the detailed experimental studies of Lieuwen and Yang [6], Kiesewetter *et al.* [7], Umeh *et al.* [8], Durox *et al.* [9], and Candel *et al.* [10]. This flame stabilization is achieved with the use of an upstream fuel injector with guiding vanes to generate swirl and a geometrical expansion of the combustion chamber. The expansion forces a corner recirculation zone near the expansion plane and causes a decrease in axial velocity in the incoming vortex core. When the swirl is sufficiently high, the vortex flow naturally breaks down in the combustion chamber, forming a centerline recirculation (breakdown) zone in addition to the corner recirculation zone. The centerline breakdown zone slows down the flow to form a chemical reaction and thereby serves as a natural aerodynamic flame holder. The reaction products are trapped in this zone and form a region of higher temperature. Heat transfer from this hot region to the surrounding expanding swirling flow helps to ignite any unreacted fuel-air pockets

*Corresponding author: rusakz@rpi.edu

from the incoming flow, support and stabilize the reaction zone, and also improve combustion effectiveness.

Vortex breakdown zones, however, also exhibit the natural appearance of precessing spiral flow instabilities inside the large recirculation zone and in its wake, and these can cause combustion dynamics, severe pressure fluctuations, and structural vibrations and affect the system performance; see the experimental investigations of Gupta *et al.* [11], Kiesewetter *et al.* [7], O'Connor and Lieuwen [12], O'Connor *et al.* [13], and Roy *et al.* [14]. Moreover, at certain operational conditions, the centerline breakdown zone may become either unstable, disappear and induce flame blowout or move upstream toward the injector, thereby posing the risk of flame flashback. These flow-axisymmetric and three-dimensional instabilities may happen spontaneously as a result of increase of swirl above a critical level. This is supported by the stability theories of Wang and Rusak [15,16], Wang *et al.* [17], and Feng *et al.* [18] for inert flows and by Choi *et al.* [19] and Rusak *et al.* [20] for reacting flows. In addition, instabilities may appear as a result of various reasons such as changes in the distribution of incoming swirl, variations of the temperature field, large vortical perturbations from the inlet, or high back pressure at the downstream end of the chamber.

The nature of reacting swirling flows with a centerline vortex breakdown zone and chamber expansion was also studied extensively in the numerical simulations of Grinstein and Fureby [21], Grinstein *et al.* [22], Lu *et al.* [23], Huang and Yang [24], Huang *et al.* [25], Franzelli *et al.* [26], and Kalis *et al.* [27]. These investigations demonstrated the existence of a large central recirculation zone in the swirling reacting flow and the resulting flame stabilization. They established the velocity, temperature and species fields in the chamber and determined the interaction of combustion dynamics, acoustic forcing, and flow instabilities at various levels of swirl and equivalent ratio.

Theoretical studies of the dynamics of reacting compressible flows with swirl and vortex breakdown were conducted by Rusak *et al.* [28], Choi *et al.* [19], and Rusak *et al.* [20]. They highlighted the natural strong nonlinear interaction between advection of azimuthal vorticity and the baroclinic effects resulting from the coupling between the swirl and the axial temperature gradient generated by the chemical reaction. The global analysis methodology of Rusak *et al.* [20] formed an analytical model problem for predicting the critical swirl level for the first spontaneous appearance of breakdown zones in a reacting flow with swirl and the size of these zones as a function of the inlet swirl level and reaction exothermicity. The theoretical predictions agree with the numerical simulations of Choi *et al.* [19].

In addition, the recent studies of Rusak and Wang [29] and Rusak *et al.* [30] have established the appearance of another type of a vortex breakdown phenomenon in inert swirling flows in pipes which results in the development of flow states with wall-separation zones. When swirl is sufficiently high the flow near the chamber wall may decelerate significantly by a certain mode of instability and above a certain critical swirl level an infinitesimally small flow flux with swirl near the wall expands into a large, quasistagnant zone attached to the pipe wall [30]. The size of this zone increases with the increase of the inlet swirl level. Moreover, while chamber divergence promotes the appearance of centerline breakdown states, it was found that chamber contraction promotes the appearance of wall-separation states to lower levels of inlet swirl, even before the formation of vortex breakdown states [30]. The recent experiments of Dennis *et al.* [31] demonstrated the existence of wall-separation states in inert flows.

The present study investigates the formation of low-Mach-number, lean premixed reacting swirling flows with wall-separation zones in a contracting circular finite-length open chamber. Figure 1 provides a schematic model of the reacting flow nature. The incoming lean premixed flow of air and fuel is injected with swirl into a finite-length circular chamber. At sufficiently high levels of the incoming flow swirl ratio, wall-separation zones are formed in the flow. The incoming flow flux of the reactants slows down to zero velocity at the leading point of the wall zone and is then deflected radially toward the centerline, thereby forming a thin reaction zone (the red line). The wall-separation zone serves as a natural aerodynamic flame holder. The reaction products are trapped in this zone and form a region of higher temperature. Heat transfer from this hot wall zone to the surrounding expanding swirling flow may help to ignite any unreacted fuel air from the incoming flow, support and stabilize the reaction zone, and improve combustion effectiveness. To

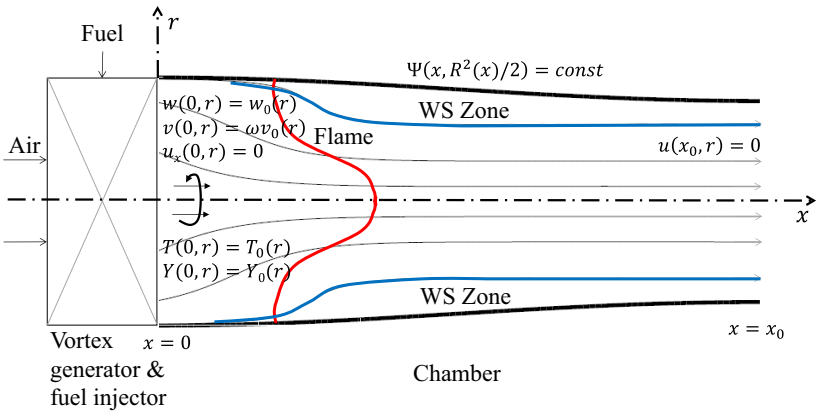

FIG. 1. Schematic diagram of a premixed reacting swirling flow with a wall-separation zone in an open contracting circular chamber.

the best of our knowledge, this proposed methodology of combustion with swirl is unique to our paper.

The main objective of the paper is to show a theoretical existence of steady combustion states in swirling flows in contracting pipes, including states of combustion with specifically a wall-separation zone. Such a solution has its own scientific merit.

The present model is limited in scope with respect to an applied case of an industrial burner. The analysis focuses on a simplified one-step chemistry model which neglects much of the details of combustion kinetics. The primary parameter of the model is the nondimensional exothermicity represented by a term $\beta\delta$. This parameter relates the temperature behind the reaction zone T_b to the inlet temperature T_a, $T_b = (1 + \beta\delta)T_a$. In the case of typical jet-engine combustion chambers with hydrocarbon-oxygen combustion $T_a \sim 800$ K and T_b is between 1600 K (corresponding to $\beta\delta = 1$) and 2400 K (corresponding to $\beta\delta = 2$). These situations demonstrate relevance of the present analysis to realistic conditions when $\beta\delta$ is between 1 and 2. We note that in laboratory experiments where $T_a = 300$ K and $T_b = 2400$ K, the exothermicity $\beta\delta$ may reach higher values near seven.

We note that detailed simulations of the various flow states and comparison with the model predictions will help to further support the ideas and provide details of the flow in the bulk. However, such simulations require a dedicated complicated solver that can resolve both the flow and the combustion structures and needs extensive and long computations.

The outline of the paper is as follows. Assuming a complete reaction with high activation energy and chemical equilibrium behind the reaction zone, the analysis uses the theory of Rusak *at el.* [20] to form a nonlinear partial differential equation for the solution of the flow stream function behind the reaction zone in terms of the specific total enthalpy for a reacting flow, the specific entropy and the circulation functions prescribed at the chamber's inlet (Sec. II). The problem is then reduced to the case of an axially independent (columnar) flow to describe the outlet state of a flow in an open chamber (Sec. III). Four types of solutions of the resulting ordinary differential equation for the columnar flow case describe the outlet state of the flow in a long chamber (Sec. IV). The approach is applied to a model case of an inlet solid-body rotation flow with uniform profiles of the axial velocity, temperature, and mixture reactant mass fraction. The bifurcation diagrams of steady flows as the inlet swirl level is increased at fixed chamber contraction and reaction heat release are described. The computed results provide theoretical predictions of the critical inlet swirl levels for the first appearance of wall-separation states and for the size of the separation zone as a function of the inlet swirl ratio, Mach number, chamber contraction and heat release of the reaction (Sec. V). The methodology developed in this paper provides a theoretical feasibility for the development of the technology of swirl-assisted combustion where the reaction zone is supported and stabilized by a wall-separation zone.

II. MATHEMATICAL MODEL

We consider a steady and axisymmtric, inviscid, compressible, premixed reacting swirling flow of a perfect gas in a contracting circular finite-length open chamber. The chamber inlet radius is $\tilde{r}$ and its length is $\tilde{l}$. We use a cylindrical coordinate system $(\bar{x}, \bar{r}, \phi)$ where the axial and radial distances are scaled with $\tilde{r}$: $x = \bar{x}/\tilde{r},\ r = \bar{r}/\tilde{r},\ 0 \leqslant x \leqslant x_0 = \tilde{l}/\tilde{r},\ 0 \leqslant r \leqslant R(x)$, and $0 \leqslant \phi < 2\pi$. The chamber shape function is given by $r = R(x) = 1 + \sigma R_0(x)$ for $0 \leqslant x \leqslant x_0$ where $\sigma \leqslant 0$ is a measure of the chamber contraction, $R_0(x)$ is a general monotonic continuous function with $R_0(0) = 0,\ R_0(x_0) = 1$, and $dR_0/dx(x_0) = 0$. For example, in the schematic diagram in Fig. 1, $R_0(x) = 1/2\{1 + \sin[\pi(x/x_0 - 1/2)]\}$ and $\sigma = -0.2$. We also assume the pipe is fully insulated in terms of heat conduction along the wall.

We assume a reacting flow with constant thermo-physical parameters. The flow properties are nondimensionalized with respect to the characteristic inlet flow properties, i.e., the radial, circumferential, and axial velocity components (u, v, w) with respect to the inlet flow centerline axial velocity $\tilde{U}$, and the temperature, density, and pressure are normalized with respect to the flow inlet centerline temperature $\tilde{T}$, density $\tilde{\rho}$, and pressure $\tilde{p}$, respectively, where $\tilde{p} = \tilde{\rho} R \tilde{T}$ and R is the specific gas constant of the reactants mixture and is assumed to be constant. In the present study, we focus on the case of a low-Mach-number combustion, $0 < \mathrm{Ma}_0 \ll 1$, where $\mathrm{Ma}_0 = \tilde{U}/\tilde{a}$ and $\tilde{a} = \sqrt{\gamma R \tilde{T}}$ is the isentropic frozen acoustic speed of sound at the inlet reference state. Here γ is the specific heat ratio ($\gamma = C_p/C_v$) and is assumed to be constant. The reactant mass fraction is Y. We assume the reaction rate W is given by a one-step first-order Arrhenius kinetics, $W = \mathscr{A} \rho Y \exp(-\frac{\theta}{T})$ where $\mathscr{A}$ is the scaled frequency factor, and θ is the scaled activation energy and both are constant. A reaction with a high activation energy θ is considered where the high-θ asymptotic approach is applicable. Then the reaction front is a thin zone and the reaction rate W is a localized function around the reaction zone. We assume a flow with a high Péclet number $\mathrm{Pe} \gg 1$ such that the diffusion and heat conduction terms in the species and energy equations may be neglected outside of the reaction zone. A complete reaction with chemical equilibrium behind the reaction zone is also considered.

Let $y = r^2/2$. In the axisymmetric flow case, a stream function $\Psi(x, y)$ is defined such that $w = \Psi_y/\rho$ and $u = -\Psi_x/(\sqrt{2y}\rho)$. Moreover, the circulation function is $K = \sqrt{2y}v$, the specific total enthalpy function (scaled with $C_p\tilde{T}$) is $H = T + \frac{(\gamma-1)\mathrm{Ma}_0^2}{2}(u^2 + v^2 + w^2)$, and the specific entropy function s (scaled with C_v) is given by Gibbs equation [32]. Under the above assumptions, Rusak *et al.* [20] have shown that the circulation, specific total enthalpy and specific entropy are functions of Ψ only, and that the flow in the chamber domain may be described by a single partial differential equation for the solution of $\Psi(x, y)$,

$$(\gamma - 1)\mathrm{Ma}_0^2\left[\frac{1}{\rho}\left(\frac{\Psi_y}{\rho}\right)_y + \frac{1}{2y\rho}\left(\frac{\Psi_x}{\rho}\right)_x\right] = H'(\Psi) - (\gamma - 1)\mathrm{Ma}_0^2\frac{K(\Psi)K'(\Psi)}{2y} - \frac{1}{\gamma}Ts'(\Psi). \quad (1)$$

Here $(\cdot)'$ represents the derivative with respect to Ψ. The temperature T and density ρ are found from the solution of the specific total enthalpy and entropy equations,

$$T = H(\Psi) - \frac{(\gamma - 1)\mathrm{Ma}_0^2}{2}\left[\frac{\Psi_x^2}{2y\rho^2} + \frac{\Psi_y^2}{\rho^2} + \frac{K^2(\Psi)}{2y}\right], \quad (2)$$

$$\rho = \left\{\frac{T}{\exp[s(\Psi)]}\right\}^{1/(\gamma-1)}. \quad (3)$$

For a flow in a finite-length circular chamber of nondimensional length x_0, we consider the following boundary conditions; see the setup in Fig. 1. At the chamber inlet, $x = 0$, the profiles of the axial velocity, the circumferential velocity, the axial derivative of radial velocity, the temperature,

and the mass fraction of the premixed reactant are given by

$$w(0, y) = w_0(y),\ v(0, y) = \omega v_0(y),\ u_x(0, y) = 0,\ T(0, y) = T_0(y),\ Y(0, y) = Y_0(y) \quad (4)$$

for $0 \leqslant y \leqslant 1/2$. Here ω is the swirl ratio of the incoming flow. It is assumed that the inlet conditions are generated by a fuel injector with a vortex generator, that mixes fuel and oxidizer ahead of the chamber and is at a continuous and steady operation. The condition $u_x(0, y) = 0$ allows a degree of freedom at the inlet to develop a radial velocity in order to model the upstream influence of disturbances in the flow. These inlet conditions may represent the flow behind a vane guide vortex generator in a fuel injector as found in the experiments of Gupta *et al.* [1,11] and Umeh *et al.* [8].

The outlet flow is assumed to be x-independent (parallel columnar) state at $x = x_0$,

$$\Psi_x(x_0, y) = K_x(x_0, y) = T_x(x_0, y) = 0 \quad \text{for} \quad 0 \leqslant y \leqslant y_e = \frac{(1+\sigma)^2}{2}. \quad (5)$$

These outlet conditions are appropriate for a sufficiently long open chamber, where the flow behind the reaction zone settles on a parallel (columnar) state at a large distance from the inlet and ahead of the outlet; see the experiments of Umeh *et al.* [8].

Along the pipe centerline at $y = 0$, the axisymmetry assumption requires $\Psi(x, 0) = 0$ for $0 \leqslant x \leqslant x_0$. The pipe rigid wall is also assumed to be adiabatic. Along the pipe wall, $y = \frac{R^2(x)}{2}$, Ψ is constant and there is no heat conduction,

$$\Psi\left(x, \frac{R^2(x)}{2}\right) = \Psi_w, \quad T_n\left(x, \frac{R^2(x)}{2}\right) = 0 \quad \text{for} \quad 0 \leqslant x \leqslant x_0. \quad (6)$$

Here n is the normal distance to the curve of the wall.

Within the high-θ asymptotic approach, W is localized around the thin reaction zone and exponentially small everywhere else. Accordingly, for the premixed reactant flow ahead of the thin reaction zone with chemical equilibrium,

$$K = K_0(\Psi), \quad Y = Y_0(\Psi), \quad H = H_0(\Psi), \quad s = s_0(\Psi). \quad (7)$$

The functions $K_0(\Psi)$, $H_0(\Psi)$, $s_0(\Psi)$, and $Y_0(\Psi)$ are determined by the inflow profiles; see Sec. III for more details.

In the flow domain behind the thin reaction zone and ahead of the pipe outlet, it is assumed that the chemical reaction has been fully completed, $W = 0$ and $Y = 0$, and the reaction product is at chemical equilibrium. We find that

$$K = K_0(\Psi), \quad Y = 0, \quad H = H_0(\Psi) + \beta Y_0(\Psi), \quad s = s_0(\Psi) + \Delta s(\Psi), \quad (8)$$

behind the reaction zone. Here β is the nondimensional heat release of the reaction, scaled by $C_p \tilde{T}$. In formulating (8), we use the fact that across the reaction zone the specific total enthalpy is increased by $\beta Y_0(\Psi)$ as a result of complete reaction of the incoming reactants. Also, $\Delta s(\Psi)$ is the increase of entropy across the thin reaction zone. In the low-Mach-number flow case $\rho \sim 1/T$ and

$$\Delta s(\Psi) = \gamma \ln\left[1 + \frac{\beta Y_0(\Psi)}{T_0(\Psi)}\right]. \quad (9)$$

The functions $K(\Psi)$, $H(\Psi)$, and $s(\Psi)$ are defined in the range of $0 \leqslant \Psi \leqslant \Psi_w$. In addition, to accommodate possible solutions with separation zones, we assume that

$$\begin{aligned} &K(\Psi) = K(0) = 0,\ H(\Psi) = H(0) = H_0,\ s(\Psi) = s(0) = s_0, \\ &K'(\Psi) = H'(\Psi) = s'(\Psi) = 0 \text{ when } \Psi < 0, \text{ and} \end{aligned} \quad (10)$$

$$\begin{aligned} &K(\Psi) = K(\Psi_w) = K_w,\ H(\Psi) = H(\Psi_w) = H_w,\ s(\Psi) = s(\Psi_w) = s_w, \\ &K'(\Psi) = H'(\Psi) = s'(\Psi) = 0 \text{ when } \Psi > \Psi_w. \end{aligned} \quad (11)$$

For a sufficiently long chamber ($x_0 \gg 1$), the flow nature in the chamber as described by the PDE (1) is dictated by the outlet state with functions according to (8) and (9). Since the outlet flow is columnar and with no radial velocity, the flow becomes asymptotically columnar as the outlet is approached and with zero reactant mass fraction.

III. THE COLUMNAR STATE

In order to determine the possible outlet states of the low-Mach-number reacting flow, we study the columnar state problem according to (1). We first determine the relationships among the properties of a base nonreacting columnar state with the axial velocity $w = w_0(y)$, the circumferential velocity $v = \omega v_0(y)$, the temperature $T = T_0(y)$, the pressure $p = p_0(y)$, and the density $\rho = \rho_0(y)$. Following Rusak *et al.* [20], we find that the base flow pressure, density, stream function, and entropy are

$$p_0(y) = \exp\left[\frac{\gamma \mathrm{Ma}_0^2 \omega^2}{2} \int_0^y \frac{{v_0}^2(\bar{y})}{\bar{y} T_0(\bar{y})}\, d\bar{y}\right], \tag{12}$$

$$\rho_0(y) = \frac{1}{T_0(y)} \exp\left[\frac{\gamma {\mathrm{Ma}_0}^2 \omega^2}{2} \int_0^y \frac{{v_0}^2(\bar{y})}{\bar{y} T_0(\bar{y})}\, d\bar{y}\right], \tag{13}$$

$$\Psi_0(y) = \int_0^y \rho_0(\bar{y}) w_0(\bar{y}) d\bar{y}, \tag{14}$$

$$s_0(y) = \gamma \left\{\ln\left[T_0(y)\right] - \frac{(\gamma - 1)\mathrm{Ma}_0^2 \omega^2}{2} \int_0^y \frac{{v_0}^2(\bar{y})}{\bar{y} T_0(\bar{y})}\, d\bar{y}\right\}. \tag{15}$$

Since $\Psi_0(y)$ is a monotonic function, this function can be inverted such that $y = y(\Psi_0)$. Then we can determine

$$K_0(\Psi_0) = \omega \sqrt{2 y(\Psi_0)}\, v_0[y(\Psi_0)], \tag{16}$$

$$H_0(\Psi_0) = T_0[y(\Psi_0)] + \frac{(\gamma - 1){\mathrm{Ma}_0}^2}{2} \{\omega^2 {v_0}^2[y(\Psi_0)] + {w_0}^2[y(\Psi_0)]\}, \tag{17}$$

$$s_0(\Psi_0) = \gamma \left(\ln\{T_0[y(\Psi_0)]\} - \frac{(\gamma - 1)\mathrm{Ma}_0^2 \omega^2}{2} \int_0^{y(\Psi_0)} \frac{{v_0}^2(\bar{y})}{\bar{y} T_0(\bar{y})}\, d\bar{y}\right\}. \tag{18}$$

The derivatives of these functions can be calculated from (16)–(18).

Equations (16)–(18) define the functions $K_0(\Psi)$, $K_0'(\Psi)$, $H_0(\Psi)$, $H_0'(\Psi)$, $s_0(\Psi)$, and $s_0'(\Psi)$ (by replacing Ψ_0 with Ψ) for a base nonreacting columnar flow and for the flow ahead of the thin reaction zone in a reacting flow. In addition, $Y_0(\Psi) = Y_0(y(\Psi))$ and $T_0(\Psi) = T_0(y(\Psi))$.

In the columnar outlet state of a reacting flow in an open chamber (which is sufficiently far behind the reaction zone), (1) is equivalent to the following system of two, first-order, nonlinear, ordinary differential equations (ODEs) in terms of w and Ψ,

$$w_y = \frac{1}{(\gamma - 1)\mathrm{Ma}_0^2} \rho \left[H'(\Psi) - (\gamma - 1)\mathrm{Ma}_0^2 \frac{K(\Psi) K'(\Psi)}{2y} - \frac{1}{\gamma} T s'(\Psi)\right], \tag{19}$$

$$\Psi_y = \rho w, \tag{20}$$

with

$$T = H(\Psi) - \frac{(\gamma - 1)\mathrm{Ma}_0^2}{2} \left[w^2 + \frac{K^2(\Psi)}{2y}\right], \tag{21}$$

$$\rho = \left\{ \frac{H(\Psi) - \frac{(\gamma-1)\mathrm{Ma}_0^2}{2}\left[w^2 + \frac{K^2(\Psi)}{2y}\right]}{\exp\left[s(\Psi)\right]} \right\}^{1/(\gamma-1)}, \tag{22}$$

and with boundary conditions:

$$\Psi(0) = 0, \quad \Psi\left[\frac{(1+\sigma)^2}{2}\right] = \Psi_w = \int_0^{\frac{(1+\sigma)^2}{2}} \rho_0(\bar{y}) w_0(\bar{y})\, d\bar{y}. \tag{23}$$

A trivial solution of the columnar flow problem (19) and (20) is $w = w_0(y)$, $v = \omega v_0(y)$, $T = T_0(y)$ with $p = p_0(y)$, $\rho = \rho_0(y)$, $Y = 0$, and $s = s_0(y)$ given by (12)–(15), i.e., the base nonreacting columnar flow. The work of Rusak *et al.* [20] for reacting swirling flows shows that when the swirl ratio $\omega \geqslant \omega^*$ additional solutions of the nonlinear columnar flow problem exist, including vortex breakdown states, which describe the flow at the pipe exit. It is expected that a similar situation occurs in the low-Mach-number reacting flow in a contracting chamber, showing the existence of multiple solutions of the problem (19)–(22) with conditions (23) and the appearance of vortex breakdown and wall-separation states. The ODEs problem (19)–(23) is solved using a standard fourth-order Runge-Kutta integration scheme and iterations until the centerline and wall conditions are satisfied. In all the examples shown below, we use $\gamma = 1.4$ and an inlet Mach number $\mathrm{Ma}_0 = 0.001$. Also, we consider an inlet solid-body rotation flow $v_0(y) = \sqrt{2y}$ with a constant unit axial velocity $w_0(y) = 1$ and constant unit temperature $T_0(y) = 1$. Also, the inlet reactant mass fraction is constant, $Y_0(y) = \delta$ where $0 \leqslant \delta < \delta_{\mathrm{st}}$ and δ_{st} is the stoichiometric reactant mass fraction.

IV. SOLUTION TYPES

The ODEs problem (19)–(23) may have several solution types, which describe the flow state at the chamber exit and determine the nature of the flow in the chamber. We focus here on solutions relevant for reaction in a contracting chamber. Figure 2 shows representative examples of the variation of the stream function Ψ, the axial velocity w, the density ρ and the temperature T as a function of y of the various types of solutions. Here we consider a constant inlet reactant mass fraction $Y_0 = \delta$, and various values of exothermicity $\beta\delta$, in a chamber with contraction parameter $\sigma = -0.2$ (at the exit $y_e = 0.32$ and radius is $r_e = 0.8$). Figure 2(a) presents the solution of a centerline accelerated flow for the case with $\sigma = -0.2$, $\beta\delta = 1$, and an inlet swirl ratio $\omega = 4$. The stream function Ψ increases monotonically with y, w has a centerline value $w(0) > 1 + \beta\delta$ and decreases monotonically with y but stays positive in the whole range $0 \leqslant y \leqslant 0.32$, while the temperature and density stay nearly constant, $T \sim 2$ and $\rho \sim 1/2$. In this type of solution, $w(0)$ is unknown and is found through iterations such that the wall condition is satisfied.

With increasing the inlet swirl ratio ω, while σ and $\beta\delta$ are fixed, there exists a certain critical swirl ratio ω_{WS}, that is a function of σ and $\beta\delta$, for which the axial velocity on the wall vanishes, $w(y_e) = 0$. We find that $\omega_{\mathrm{WS}} = 4.69$ when $\sigma = -0.2$ and $\beta\delta = 1$. For $\omega > \omega_{\mathrm{WS}}$, the solutions turn into wall-separation solutions, see an example in Fig. 2(b) for the case with $\sigma = -0.2$, $\beta\delta = 1$, and $\omega = 4.8$. In this solution, the stream function Ψ increases monotonically with y in the range $0 \leqslant y < y_w = 0.226$ and $\Psi = \Psi_w$ in the range $y_w \leqslant y \leqslant y_e$. The axial velocity w decreases monotonically in the range $0 \leqslant y < y_w$ and $w = 0$ in the range $y_w \leqslant y \leqslant y_e$, while the temperature and density stay nearly constant, $T \sim 2$ and $\rho \sim 1/2$. In the wall-separation zone $y_w \leqslant y \leqslant y_e$, the axial and radial velocity components are zero, but the circumferential velocity is not zero and is given by $K(\Psi_w)/\sqrt{2y}$. In this type of solution, the interface location y_w is unknown and is found through iterations such that the centerline condition is satisfied.

With increasing exothermicity $\beta\delta$ at a fixed chamber contraction σ, there exists a limit value $(\beta\delta)_l$ where the branch of the centerline accelerated flow solutions that is followed by the wall-separation solutions ceases to exist. We find that $(\beta\delta)_l = 1.12$ for $\sigma = -0.2$. For $\beta\delta > (\beta\delta)_l$ and a fixed σ, the branch of solutions changes its nature. When ω is relatively small, the solution shows

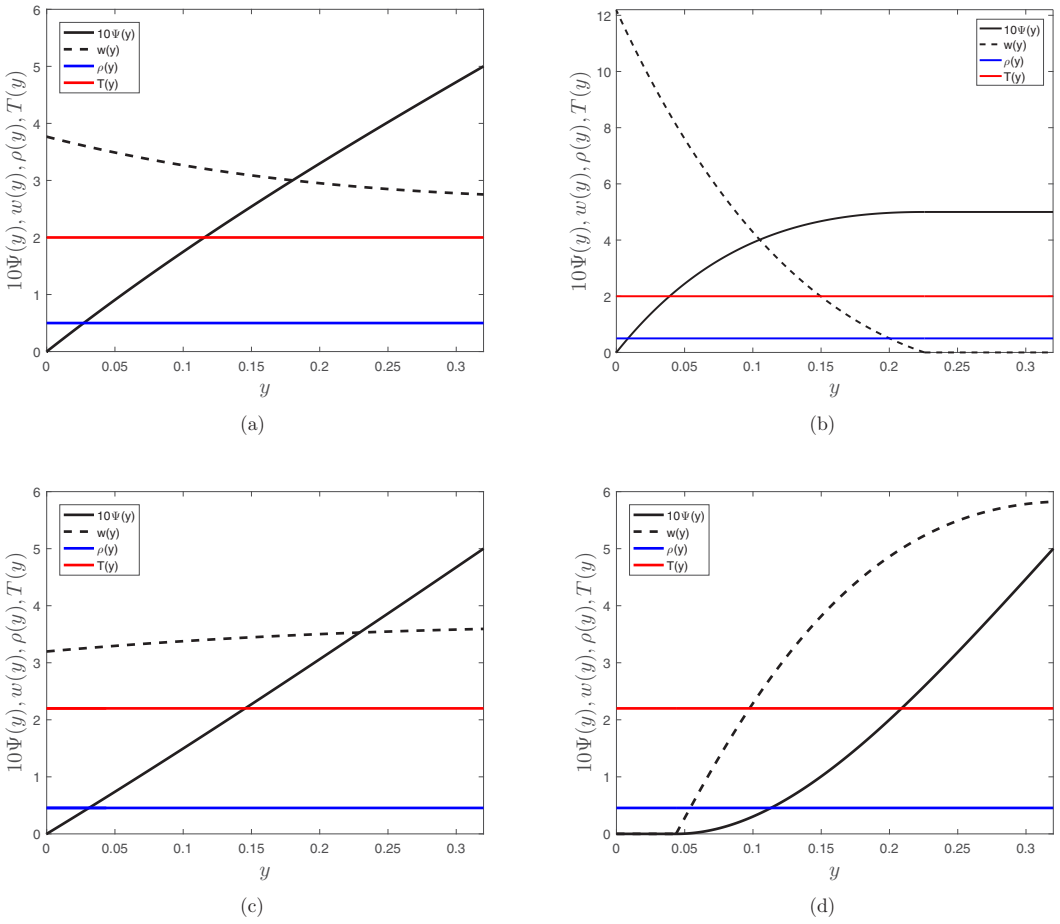

FIG. 2. The various types of solutions of the columnar problem: (a) a centerline accelerated flow state at $\sigma = -0.2,\ \beta\delta = 1,\ \omega = 4$; (b) a wall-separation state at $\sigma = -0.2,\ \beta\delta = 1,\ \omega = 4.8$; (c) a decelerated flow state at $\sigma = -0.2,\ \beta\delta = 1.2,\ \omega = 4$; (d) a vortex breakdown state at $\sigma = -0.2,\ \beta\delta = 1.2,\ \omega = 5.5$.

that the stream function Ψ increases monotonically with y, the axial velocity w is positive and increases monotonically with y while the temperature and density stay nearly constant, $T \sim 2.2$ and $\rho \sim 0.455$; see an example in Fig. 2(c) for $\sigma = -0.2$, $\beta\delta = 1.2$, and $\omega = 4$. The centerline velocity $w(0)$ decreases with increasing of ω. In this type of solution, $w(0)$ is unknown and is found through iterations such that the wall condition is satisfied.

With increasing the inlet swirl ratio ω, while σ and $\beta\delta$ are fixed, there exists a certain critical swirl ratio, ω_{BD}, that is also a function of σ and $\beta\delta$, for which the axial centerline velocity vanishes, $w(0) = 0$. We find that $\omega_{\mathrm{BD}} = 5.122$ when $\sigma = -0.2$ and $\beta\delta = 1.2$. For $\omega > \omega_{\mathrm{BD}}$, the solutions turn into vortex-breakdown solutions; see an example in Fig. 2(d) for the case with $\sigma = -0.2,\ \beta\delta = 1.2$, and $\omega = 5.5$. In this solution, the stream function $\Psi = 0$ in the range $0 \leqslant y < y_0 = 0.044$ and increases monotonically in the range $y_0 \leqslant y \leqslant y_e$. The axial velocity $w = 0$ in the range $0 \leqslant y < y_0$ and also increases monotonically in the range $y_0 \leqslant y \leqslant y_e$, while the temperature and density stay nearly constant, $T \sim 2.2$ and $\rho \sim 0.455$. In the vortex-breakdown zone $0 \leqslant y \leqslant y_0$, the axial, radial, and circumferential velocity components are zero. In this type of solution, the breakdown-zone size y_0 is unknown and is found through iterations such that the wall condition is satisfied.

These four types of solutions of the ODE problem [(19)–(23)] form the outlet states of the reacting flow with swirl in the contracting chamber. Therefore, the PDE problem [(1)–(11)] has

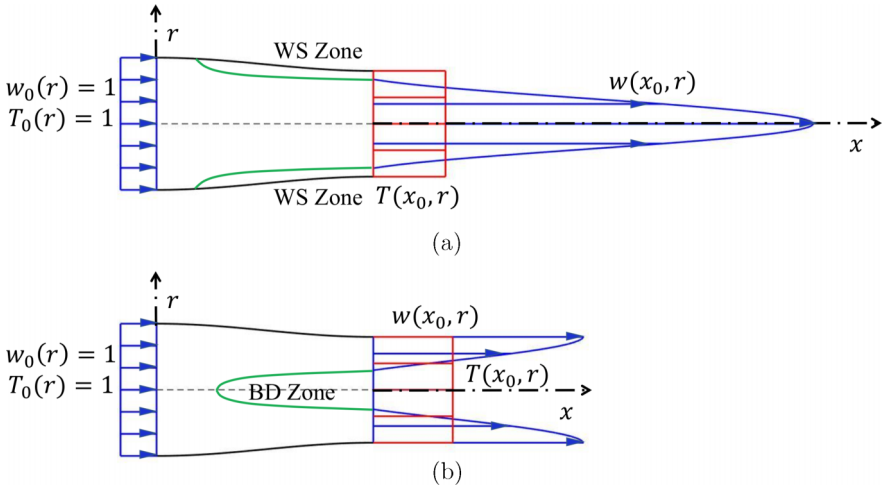

FIG. 3. Schematic diagram of axial velocity and temperature profiles at the chamber inlet and outlet: (a) a wall-separation state at $\sigma = -0.2,\ \beta\delta = 1,\ \omega = 4.8$; (b) a vortex-breakdown state at $\sigma = -0.2,\ \beta\delta = 1.2,\ \omega = 5.5$.

four types of related solutions of a reacting flow with swirl in a contracting chamber. These include the accelerated flow state all along the chamber centerline, the wall-separation state, the decelerated flow state all along the chamber centerline and the vortex-breakdown state.

We refer the reader to the detailed simulated examples of inert flow stream function in diverging or contracting pipes shown in Rusak *et al.* [30] which show nice agreement with the model predictions at the pipe outlet. In addition, a schematic description of the present results with combustion is added in Fig. 3. Figure 3(a) illustrates the inlet and outlet axial velocity and temperature of the wall-separation state for the case with $x_0 = 6,\ \sigma = -0.2,\ \beta\delta = 1$, and $\omega = 4.8$. It can be seen that the flow accelerates along the centerline and decelerates to a stagnation zone attached to the chamber wall. Figure 3(b) illustrates the inlet and outlet axial velocity and temperature of the vortex-breakdown state for the case with $x_0 = 6,\ \sigma = -0.2,\ \beta\delta = 1.2$, and $\omega = 5.5$. It can be seen that the flow decelerates along the centerline to a finite-size stagnation breakdown zone around the centerline. We conjuncture that detailed simulations of flow states with combustion will also show agreement with the model predictions.

V. RESULTS

Extensive numerical solutions of the ODE problem (19)–(23) provide the dividing line of the limit exothermivity $(\beta\delta)_l$ as a function of $\sigma < 0$ in the operational map of exothermicity $\beta\delta$ against chamber contraction parameter σ; see our results in Fig. 4. This line separates between the operational conditions where reacting flows with swirl and either centerline-accelerated flow or wall-separation zones may appear and the conditions where reacting flows with swirl and either centerline-decelerated flows or vortex-breakdown zones may appear. In the present study, we focus on reacting flow states with swirl and wall separation. It can be seen from Fig. 4 that, depending on the swirl level, such states appear when $0 < \beta\delta < (\beta\delta)_l$ for a fixed chamber contraction. For a fixed exothermicity $\beta\delta$, there is a need for a sufficient amount of chamber contraction and high swirl to generate such states. It should be noted that if chamber contraction is not sufficiently large or if the chamber is diverging ($\sigma > 0$) only reacting flows with centerline vortex-breakdown zones may appear. Chamber contraction promotes the appearance of wall-separation states in swirling flows (see Ref. [30]), while reaction causes flow acceleration to push out the wall-separation zones. The interaction between the chamber shape and reaction exothermicity determines the possibility to generate states with wall-separation zones at sufficiently high inlet swirl ratios.

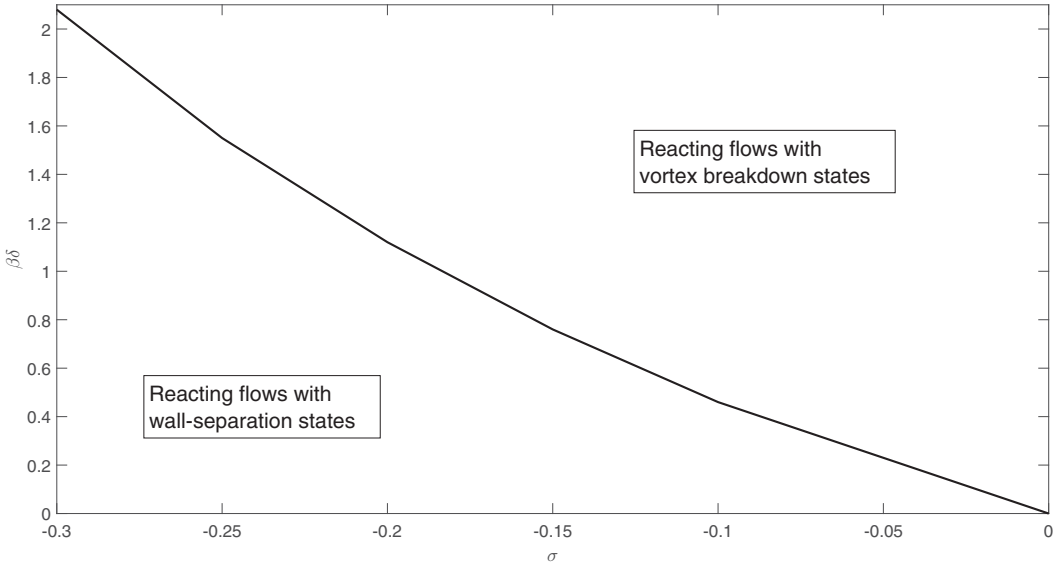

FIG. 4. The dividing line $(\beta\delta)_l$ as a function of $\sigma < 0$ separating between operational conditions where reacting flows with swirl and wall-separation zones may appear and conditions where reacting flows with swirl and vortex breakdown may appear.

Figure 5 presents the bifurcation diagram of reacting flow states with swirl for a representative example with chamber contraction $\sigma = -0.2$ and exothermicity $\beta\delta = 1$. Figure 5(a) shows the resulting outlet centerline axial velocity $w(0, x_0)$ (solid line) and the related outlet wall axial velocity $w(y_e, x_0)$ (dashed line) as a function of ω. It can be seen that $w(0, x_0)$ increases with ω while $w(y_e, x_0)$ decreases with ω. At the critical swirl ratio $\omega = \omega_{\rm WS} = 4.69$ reacting flows with wall-separation zones appear. Figure 5(b) describes the resulting radial location at the chamber outlet of the interface of the wall-separation zone y_w as a function of ω. It is found that y_w decreases and the wall-separation zone increases in size with increasing ω above $\omega_{\rm WS}$.

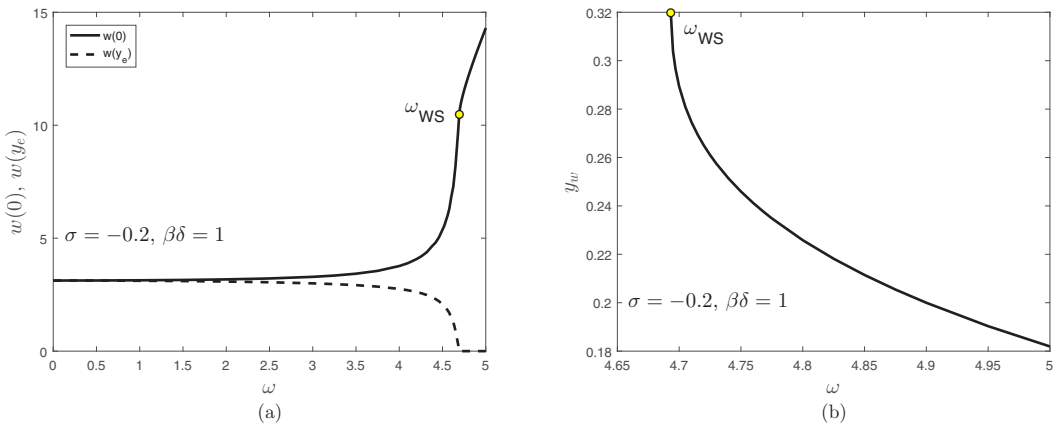

FIG. 5. The diagrams of main parameters of reacting flow states with swirl for $\sigma = -0.2$ and $\beta\delta = 1$. (a) The centerline axial velocity $w(0)$ (solid line) and related wall axial velocity $w(y_e)$ (dashed line) as a function of ω. (b) The resulting location of the interface of the wall-separation zone y_w as a function of ω. The circles mark the swirl ratio $\omega_{\rm WS}$ for the first appearance of wall-separation states.

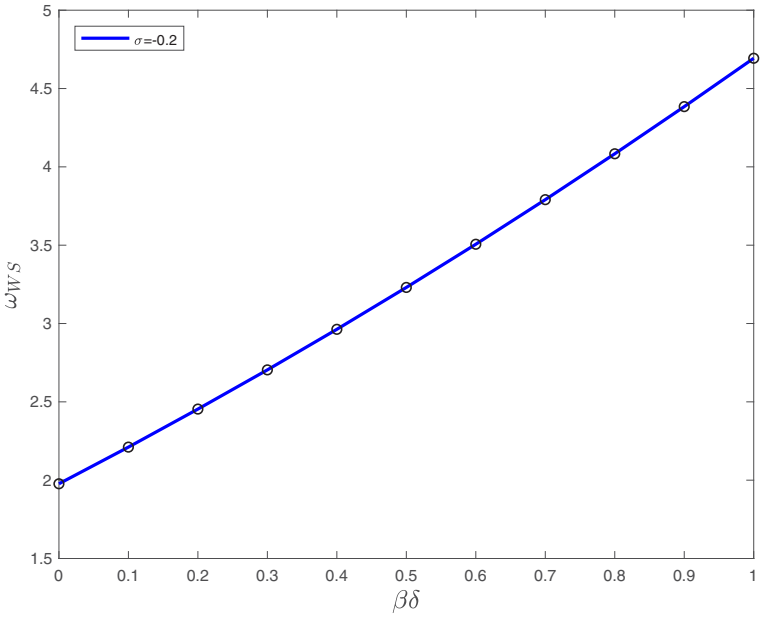

FIG. 6. The critical swirl ratio $\omega_{\rm WS}$ for the first appearance of wall-separation states as a function of exothermicity $\beta\delta$ for contracting chambers with $\sigma = -0.2$.

The critical swirl ratio $\omega_{\rm WS}$ for the first appearance of wall-separation states as a function of exothermicity $0 < \beta\delta \leqslant 1$ for a contracting chamber with $\sigma = -0.2$ is shown in Fig. 6. The higher the reaction exothermicity is or the greater chamber contraction is, the higher the critical swirl ratio is. Figures 4 and 6 together complete the information of operational conditions in terms of ω, $\beta\delta$ and σ needed for establishing reacting flows with swirl and wall-separation zones.

VI. CONCLUSIONS

This paper establishes the theoretical feasibility of generating low-Mach-number, lean premixed reacting swirling flows with wall-separation zones in a contracting circular finite-length open chamber; see Fig. 1. The study is based on a global analysis methodology of the nonlinear partial differential equation that describes such flows. The approach is applied to a model problem with complete reaction, high activation energy, and chemical equilibrium behind the reaction zone. Also, the model considers an inlet solid-body rotation flow with constant profiles of the axial velocity, temperature and mixture reactant mass fraction. Four types of solutions of the problem are found; see Fig. 2. The computed results clarify the range of operational conditions in terms of the inlet swirl ratio ω, the chamber contraction $\sigma < 0$ and the reaction exothermicity $\beta\delta$ for the existence of such states; see Figs. 4 and 6. Sufficient chamber contraction promotes the appearance of wall-separation states while reaction exothermicity and chamber divergence promote the appearance of reacting flows with swirl and vortex-breakdown states. Sufficiently high swirl is needed for reacting flows with wall-separation zones.

The idea of establishing reacting flows with swirl and wall-separation zones that stabilize the reaction zone was never studied in numerical simulations or in experimental models. With respect to the concept of reaction with centerline vortex-breakdown zones and chamber divergence, this idea may have the advantage of a greater capture area of the premixed reactants near the wall. The contracting chamber uses a more compact configuration. The resulting higher axial velocity around the outlet centerline adds kinetic energy to the high thermal energy and can be used to drive the turbine behind the combustor in either a power generation system or a jet engine. Developing this

concept of combustion with swirl and demonstrating its practicality requires additional theoretical modeling, detailed numerical simulations and extensive experimental studies.

[1] A. K. Gupta, D. G. Lilley, and N. Syred, *Swirl Flows* (Abacus Press, Tunbridge Wells, England, 1984), p. 488.

[2] A. H. Lefebvre, *Gas Turbine Combustion*, second edition (CRC Press, Taylor and Francis group, Boca Raton, Florida, 1998).

[3] S. Sivasegaram and J. Whitelaw, The influence of swirl on oscillations in ducted premixed flames, Combust. Flame **85**, 195 (1991).

[4] C. O. Paschereit, E. Gutmark, and W. Weisenstein, Control of thermoacoustic instabilities and emissions in an industrial-type gas-turbine combustor, in *27th Symp. (International) on Combustion* (Combustion Institute, 1998), Vol. 27, pp. 1817–1824.

[5] C. O. Paschereit, E. Gutmark, and W. Weisenstein, Excitation of thermoacoustic instabilities by interaction of acoustics and unstable swirling flow, AIAA J. **38**, 1025 (2000).

[6] T. Lieuwen and V. Yang, *Combustion Instabilities in Gas Turbine Engines: Operational Experience, Fundamental Mechanisms, and Modeling*, Progress in Astronautics and Aeronautics (American Institute of Aeronautics and Astronautics, Reston, Virginia, 2005).

[7] F. Kiesewetter, M. Konle, and T. Sattelmayer, Analysis of combustion induced vortex breakdown driven flame flashback in a premix burner with cylindrical mixing zone, J. Eng. Gas Turbines Power **129**, 929 (2007).

[8] C. O. Umeh, Z. Rusak, and E. Gutmark, Vortex breakdown in a swirl-stabilized combustor, J. Propul. Power **28**, 1037 (2012).

[9] D. Durox, J. P. Moeck, J.-F. Bourgouin, P. Morenton, M. Viallon, T. Schuller, and S. Candel, Flame dynamics of a variable swirl number system and instability control, Combust. Flame **160**, 1729 (2013).

[10] S. Candel, D. Durox, T. Schuller, J.-F. Bourgouin, and J. P. Moeck, Dynamics of swirling flames, Annu. Rev. Fluid Mech. **46**, 147 (2014).

[11] A. Gupta, M. Lewis, and S. Qi, Effect of swirl on combustion characteristics in premixed flames, J. Eng. Gas Turbines Power **120**, 488 (1998).

[12] J. O'Connor and T. Lieuwen, Recirculation zone dynamics of a transversely excited swirl flow and flame, Phys. Fluids **24**, 075107 (2012).

[13] J. O'Connor, V. Acharya, and T. Lieuwen, Transverse combustion instabilities: Acoustics, hydrodynamics, and flame dynamics, Prog. Energy Combust. Sci. **49**, 1 (2015).

[14] S. Roy, T. Yi, N. Jiang, G. Gunaratne, I. Chterev, B. Emerson, T. Lieuwen, A. Caswell, and J. Gord, Dynamics of robust structures in turbulent swirling reacting flows, J. Fluid Mech. **816**, 554 (2017).

[15] S. Wang and Z. Rusak, On the stability of an axisymmetric rotating flow in a pipe, Phys. Fluids **8**, 1007 (1996).

[16] S. Wang and Z. Rusak, The dynamics of a swirling flow in a pipe and transition to axisymmetric vortex breakdown, J. Fluid Mech. **340**, 177 (1997).

[17] S. Wang, Z. Rusak, R. Gong, and F. Liu, On the three-dimensional stability of a solid-body rotation flow in a finite-length rotating pipe, J. Fluid Mech. **797**, 284 (2016).

[18] C. Feng, F. Liu, Z. Rusak, and S. Wang, Dynamics of a perturbed solid-body rotation flow in a finite-length straight rotating pipe, J. Fluid Mech. **846**, 1114 (2018).

[19] J. Choi, Z. Rusak, and A. Kapila, Numerical simulation of premixed chemical reactions with swirl, Combust. Theory Modell. **11**, 863 (2007).

[20] Z. Rusak, J. J. Choi, N. Bourquard, and S. Wang, Vortex breakdown in premixed reacting flows with swirl in a finite-length circular open pipe, J. Fluid Mech. **793**, 749 (2016).

[21] F. Grinstein and C. Fureby, LES studies of the flow in a swirl gas combustor, Proce. Combust. Inst. **30**, 1791 (2005).
[22] F. F. Grinstein, N.-S. Liu, and J. C. Oefelein, Introduction: Combustion modeling and large eddy simulation: Development and validation needs for gas turbines, AIAA J. **44**, 417 (2006).
[23] X. Lu, S. Wang, H.-G. Sung, S.-Y. Hsieh, and V. Yang, Large-eddy simulations of turbulent swirling flows injected into a dump chamber, J. Fluid Mech. **527**, 171 (2005).
[24] Y. Huang and V. Yang, Effect of swirl on combustion dynamics in a lean-premixed swirl-stabilized combustor, Proc. Combust. Inst. **30**, 1775 (2005).
[25] Y. Huang, S. Wang, and V. Yang, Systematic analysis of lean-premixed swirl-stabilized combustion, AIAA J. **44**, 724 (2006).
[26] B. Franzelli, E. Riber, L. Y. Gicquel, and T. Poinsot, Large eddy simulation of combustion instabilities in a lean partially premixed swirled flame, Combust. Flame **159**, 621 (2012).
[27] H. Kalis, M. Marinaki, U. Strautins, and O. Lietuvietis, On the numerical simulation of the vortex breakdown in the combustion process with simple chemical reaction and axial magnetic field, Intl. J. Differential Eq. Appl. **14**, 235 (2015).
[28] Z. Rusak, A. Kapila, and J. J. Choi, Effect of combustion on near-critical swirling flow, Combust. Theory Model. **6**, 625 (2002).
[29] Z. Rusak and S. Wang, Wall-separation and vortex-breakdown zones in a solid-body rotation flow in a rotating finite-length straight circular pipe, J. Fluid Mech. **759**, 321 (2014).
[30] Z. Rusak, Y. Zhang, H. Lee, and S. Wang, Swirling flow states in finite-length diverging or contracting circular pipes, J. Fluid Mech. **819**, 678 (2017).
[31] D. J. Dennis, C. Seraudie, and R. J. Poole, Controlling vortex breakdown in swirling pipe flows: experiments and simulations, Phys. Fluids **26**, 053602 (2014).
[32] K. Kuo, *Principles of Combustion* (John Wiley & Sons, New York, 1986).